Geoderma 207-208 (2013) 166–179

Contents lists available at SciVerse ScienceDirect

Geoderma

journal homepage: www.elsevier.com/locate/geoderma

Spatio-temporal modeling of soil characteristics for soilscape reconstruction

Ann Zwertvaegher [a], Peter Finke [a,*], Philippe De Smedt [b], Vanessa Gelorini [a], Marc Van Meirvenne [b], Machteld Bats [c], Jeroen De Reu [c], Marc Antrop [d], Jean Bourgeois [c], Philippe De Maeyer [d], Jacques Verniers [a], Philippe Crombé [c]

[a] Department of Geology and Soil Science, Ghent University, Krijgslaan 281, 9000 Ghent, Belgium
[b] Research Group Soil Spatial Inventory Techniques, Department of Soil Management, Ghent University, Coupure 653, 9000 Ghent, Belgium
[c] Department of Archaeology, Ghent University, Sint-Pietersnieuwstraat 35, 9000 Ghent, Belgium
[d] Department of Geography, Ghent University, Krijgslaan 281, 9000 Ghent, Belgium

ARTICLE INFO

Article history:
Received 13 July 2012
Received in revised form 2 May 2013
Accepted 14 May 2013
Available online xxxx

Keywords:
Process modeling
Pedogenesis
Regression kriging
Holocene

ABSTRACT

Full-coverage maps for several specific soil characteristics were produced at particular time-intervals over a time span of 12,716 years for a 584 km^2 large study area located in Belgium. The pedogenetic process model SoilGen2 was used to reconstruct the evolution of several soil variables at specific depths in the soil profile at various point locations (96 in total). The time span covered by the simulations encompassed the final part of the Younger Dryas and the Holocene up till the present. Time series on climate, organisms and groundwater table were reconstructed and supplied to the model as boundary conditions. Model quality optimization was performed by calibrating the solubility constant of calcite by a comparison of the simulated time necessary for decarbonization with literature values and evaluating the calibrated value over a wide range of precipitation surpluses representative for the regarded time period. The simulated final state was evaluated against measurements collected in a database representing the historic state of the soil at 1950. The simulated specific soil characteristics at the point locations were then used to produce full-coverage maps at the particular time-intervals by regression kriging. Such maps are believed to provide useful information for geoarcheological studies and archeological land evaluations.

1. Introduction

Since prehistoric times, man has lived in close interaction with the land, which aspects are believed to have influenced decision making on occupation and utilization of a region. For example, analyses of the spatial distribution of archeological finds and their possible correlation with physical/environmental variables were the subject of investigations since the 1970s (e.g., De Reu et al., 2011; Niknami et al., 2009). Anthropogenic activity, on the other hand, influences the environment as well (Knight and Howard, 2004; Oetelaar and Oetelaar, 2007). Usage of the land in prehistoric times encompassed not only settlement, but also the provisioning in livelihood for example through hunting and/or fishing and gathering, which was the main way of subsistence until the Mesolithic inclusive. Agriculture was practiced from the Neolithic onwards, its starting point, degree of continuity and intensity varying spatially (Crombé and Vanmontfort, 2007). Various types of pre- and protohistoric land use serving as biophysical attractors for occupation were listed by Zwertvaegher et al. (2010), together with their associated land qualities and characteristics. For example, the land utilization type rain-fed agriculture that is among other things influenced by land qualities such as moisture, oxygen and nutrient availability in the soil.

The component soil is an important factor in establishing the suitability of the land for several types of land use. Natural soil fertility is determined by the physical and chemical soil properties that are the product of several soil forming processes and are therefore variable through time. Mostly, only the present-day state of the soil is known, together with the condition of the parent material. Unless soil chronosequences are at hand, no information on past soil conditions is available (Finke, 2012). Therefore, process models using the knowledge on physical and chemical processes, are interesting tools in the reconstruction of the paleo-characteristics of the land (Zwertvaegher et al., 2010) that enable land evaluation and population carrying capacity assessment for past (pre-)historic situations. Such land evaluation can then be used to explain spatial variation in the density of soil occupation as recorded in archeological prospection (Finke et al., 2008). Concerning the factor soil, the pedogenetic process model SoilGen (Finke, 2012; Finke and Hutson, 2008) was used to provide the necessary variables for a specific time and depth of the soil profile at several point locations (Zwertvaegher et al., 2010). Currently, SoilGen is one of the few mechanistic models able to reconstruct depth profiles of soil variables such as clay content, OC content, base saturation, CEC, and pH and which was confronted to field measurements (Opolot et al.,

* Corresponding author. Tel.: +32 92644630.
E-mail address: Peter.Finke@UGent.be (P. Finke).

0016-7061/$ – see front matter © 2013 Elsevier B.V. All rights reserved.
http://dx.doi.org/10.1016/j.geoderma.2013.05.013

in review; Samouëlian et al., 2012; Sauer et al., 2012). In contrast to soil development models that do not include the water cycle (e.g., MILESD, Vanwalleghem et al., in press), effects of climate change can be accounted for with SoilGen (Finke and Hutson, 2008), which is of great relevance when paleolithic and mesolithic periods are studied. With such model as a temporal interpolator, past situations can be reconstructed, not only for geoarcheological purposes such as in this paper, but also for the estimation of carbon stock pool size evolution over multimillenniums. Additionally, such model can also be used to evaluate scenarios of soil formation at the pedon scale and the landscape scales (Finke et al., in review; Vanwalleghem et al., in press).

The main objective of this work was producing full-coverage maps of the study area of soil characteristics relevant for past human occupation at certain points in time. To attain this, the model boundary conditions and initial conditions were reconstructed for the time period at hand. Additionally, the model reliability was maximized by calibration of the model-processes and evaluation of the simulated final state by comparison with the measured final state. Finally, the model outputs at several point locations were used in the reconstruction of full-coverage maps of specific soil characteristics.

2. Study area

The study area encompasses a total of 584 km^2 and is situated in the region of Flanders, in the northern part of Belgium (Fig. 1). Archeological investigations in the Flanders region revealed areas with high-site densities, as well as areas with very little archeological evidence, despite repeated archeological surveys. The study area was chosen to encompass both of these areas, as well as a broad environmental diversity, such as dry and wet soils, and topographical gradients.

The soils of the study area are dominantly characterized by sand textures according to the Belgian classification, ranging from moderately wet to moderately dry, and loamy sand textures, with drainage classes from moderately wet to wet (Tavernier et al., 1960). This sandy substrate was largely deposited during the fluvial infilling of a valley system, called the Flemish Valley, formed during Pleistocene glacial and interglacial cycles (De Moor and van de Velde, 1995). These sediments were afterwards reworked by strong aeolian activity towards the end of the Pleniglacial and also during the Late Glacial. This resulted in the formation of parallel east-western oriented dunes and dune complexes with heights up to 10 m.a.s.l. (De Moor and Heyse, 1974; Heyse, 1979). Tertiary marine sandy and clayey layers are found in outcrops, such as the cuesta of Waas and the hills of Central West Flanders (De Moor and Heyse, 1974; Fig. 1). Calcareous gyttja infillings (marl) are present in several depressions along the southern border of the coversand dune area. The Moervaart depression is the largest of these depressions with an approximate length of 25 km (Crombé et al., 2012). In the alluvial plains of the major river valleys and in these semi-alluvial depressions, sand loam, clay and peat are also found. These are associated with wet to very wet, and even extremely wet locations (Tavernier et al., 1960). A distinct soil profile development is generally absent in these soils (Tavernier et al., 1960; Van Ranst and Sys, 2000).

Regosols and Arenosols found in sandy textures with excessive drainage are often due to recent sediment movement and redeposition in dune contexts (Van Ranst and Sys, 2000). In these cases, a buried Podzol is often found at a certain depth (Ameryckx, 1960). Several other stages of soil profile development in the more sandy textures are found in the study region, corresponding with WRB classified Cambisols, Albeluvisols and Podzols(IUSS Working Group WRB, 2006). Plaggic Anthrosols also occur in the study area, as

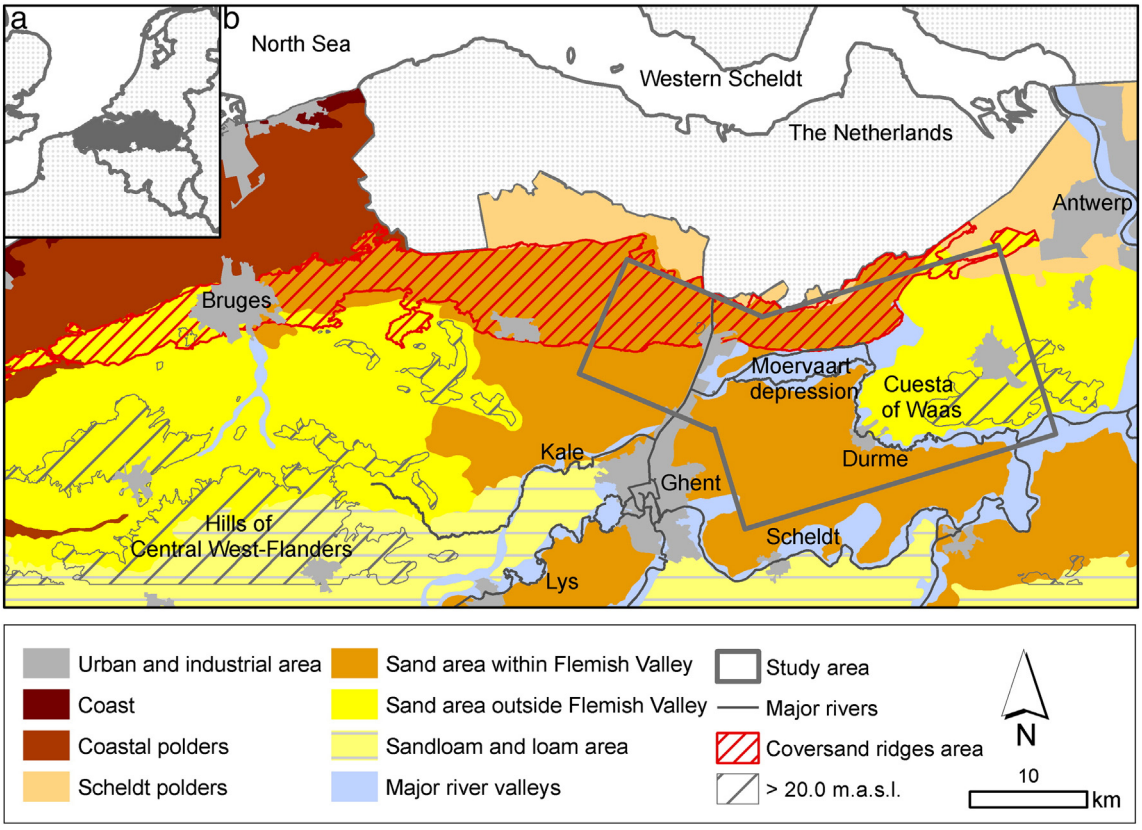

Fig. 1. a: Localization of Flanders (indicated in gray) within Belgium; b: localization of the study area within the northern part of Flanders, showing the main landscapes and geomorphological features. The delineated (hatched) entities "Hills of Central West-Flanders" and "Cuesta of Waas" consist of sediments of Tertiary age, other entities are of Quaternary age.

the result of long-term human plaggen management, which was fully established since the Middle Ages (Blume and Leinweber, 2004). Heath sods and/or forest litter were used as bedding material to the stables. Occasionally, the bedding was removed and applied to the cultivated land as manure (FAO, 2001; Sanders et al., 1989). As a side-effect the land was heightened over time and lowered at the location were the original sods were removed.

The soil formation in a region stands in close interaction with its vegetation development. This information was provided through the palynological research of Verbruggen (1971) and Verbruggen et al. (1996). Chronozones and conceptualized vegetation types are depicted in Fig. 4. The Younger Dryas was characterized by a decline of the pine-birch (*Pinus–Betula*) forest and the expansion of the herbaceous vegetation. From the Holocene onwards, the forest regenerated due to the ameliorating climatic conditions. This started with the increasing and eventually dominating presence of birch. A short temperature oscillation during the Preboreal was accompanied with the sudden increase in *Gramineae* (grasses) (Verbruggen, 1971). Afterwards, the presence of pine increased leading to the construction of an almost closed pine–birch forest. From the beginning of the Boreal, hazel (*Corylus*) occurred and later on also oak (*Quercus*) and elm tree (*Ulmus*). This was the onset towards the mixed-oak (*Quercetum mixtum*) forest, which was fully established from the Atlantic onward (Verbruggen, 1971) and was especially present on the dryer grounds, while alder (*Alnus*) occupied the wetter parts (Verbruggen et al., 1996). Lime (*Tilia*) and elm (*Ulmus*) declined from the transition to the Subboreal onward, while the presence of beech (*Fagus sylvaticus*) gradually increased and the first human impacts on the vegetation can be observed in the pollen diagrams (Verbruggen, 1971; Verbruggen et al., 1996). Initially, this started with very small open spots in the forest. Only in the coversand area the forest was degraded, resulting in grassland with hazel and birch, and later on heathland with birch. Systematic clearances appeared from the Roman Ages onwards, although a slight regeneration of the forest was observed during the medieval times. Afterwards, however, the final clearances took place with the removal of the last patches of natural vegetation and the establishment of the cultural landscape.

3. The Soilgen model

The SoilGen model (Finke, 2012; Finke and Hutson, 2008) was developed to simulate soil formation in unconsolidated sediments. In the model, a soil profile at a certain point location is represented by a number of compartments (here, taken as 0.05 m thickness). The physical and chemical soil properties are updated at varying time steps, the temporal resolution depending on the specific parameter and process dynamics. This mostly concerns the subday time scale (Finke and Hutson, 2008). In this model, the factors of soil formation as defined by Jenny (1941), are taken into account as boundary and initial conditions, as well as by several simulated processes (for an overview, see Sauer et al., 2012). Below, a general overview of the model is given; for more detailed model descriptions refer to Finke and Hutson (2008).

The SoilGen2 model core is based on the LEACHC model (Hutson and Wagenet, 1992), calculating water, solute and heat flow. These flows are governed by finite difference approximations of the Richard's equation for the unsaturated zone, the convection–dispersion equation and the heat flow equation respectively. Information on the parent material is introduced to the model as initial conditions. Physical weathering and weathering of the primary minerals is handled, as well as clay migration, which is induced by rain splash detachment at the surface bringing part of the clay particles in the dispersed state (Finke, 2012). Precipitation, potential evapotranspiration, air temperature and rainfall composition are applied to the model as boundary conditions. The influence of topography is parameterized by the slope aspect and gradient and the wind bearing (Finke, 2012). This enables the model to modify precipitation and potential evapotranspiration to local exposition properties. Furthermore, erosion and sedimentation events are also managed as input (Finke, 2012). Hydrological conditions are set using a default free drainage lower boundary, except in the occurrence of a precipitation deficit, in which case a zero flux condition is applied. Shallow water tables occurring inside the modeled soil profile, are to be supplied by the user as an extra boundary condition. When seasonal dynamics are absent in the input (for example mean water tables delivered at yearly time scale), seasonal water table fluctuations are simulated by imposing a reduced permeability at the height of the mean water table, which causes a perched water table to be simulated around the mean water table depth, responding to variations in precipitation surplus. The vegetation is conceptualized by 4 vegetation types (grass/shrubs, conifers, deciduous wood and agriculture), each with a specific root distribution pattern, ion and water uptake and release, and C-cycling (Finke, 2012; Finke and Hutson, 2008). Decomposition and mineralization of the organic matter (OM) are calculated within a C-cycling submodel of SoilGen, based on RothC 26.3 (Coleman and Jenkinson, 2005). The produced CO_2 is handled by the gas regime equation and the calculated partial pressure in its turn influences the chemical equilibria between the solution phase, the precipitated, the exchange and the unweathered phase. Human influence is modeled by fertilization and tillage. Redistribution of the several soil phases (minerals, OM, soil water and dissolved elements) by bioturbation and tillage, is mimicked by the model as an incomplete mixing process (Finke and Hutson, 2008).

The various parts of the SoilGen model that have been tested: water and solute transport (Addiscott and Wagenet, 1985; Dann et al., 2006; Jabro et al., 2006), soil chemistry (Jalali and Rowell, 2003) and carbon dynamics (Smith et al., 1997). Furthermore, the model was tested and evaluated for a wide range of parameters (Finke, 2012; Finke and Hutson, 2008; Sauer et al., 2012).

4. Reconstructing model boundary conditions at the point location

4.1. Available data

The Belgian soil was systematically mapped (1/20,000 based on 2 samples per ha) during the national soil survey campaign, initiated in 1947. During the campaign, additional soil profile descriptions, horizon sampling and analyses were performed. The major part of these data (13,000 profiles) was stored in the Aardewerk database (Van Orshoven et al., 1988, 1993), containing a total of 53 variables (Van Orshoven et al., 1988). These concern the identification and characterization of the profiles and their associated horizons, for instance granulometry, organic carbon (OC), pH(H_2O), pH(KCl), cation exchange capacity (CEC), exchangeable cations, free iron and mineralogy of the sand fraction (Dudal et al., 2005). The information from this database was used to assess the initial soil state. Furthermore, it represents the final state of the soil, necessary for model evaluation.

A total of 390 profiles from the Aardewerk database are situated inside the study area (Fig. 2). The soil development reconstruction was performed on 96 locations. These were manually selected to cover the regional ranges in texture and drainage class in accordance to their areal percentages. Furthermore, the locations were chosen to independently and uniformly cover the entire study area. This was visually confirmed by a Complete Spatial Randomness (CSR) test in which the actual distribution of coordinates was plotted against the expected distribution of a CSR.

However, certain inconsistencies were found in the original Aardewerk database, which were firstly removed. Profile layers with total fine earth not equal to 100%, were assigned the fine earth fractions of the adjoining layer with the highest similarity in OC and calcite contents. Furthermore, OC contents of 0.0% for recorded peat layers were adjusted to a fixed value of 70.0% (the average value for peat layers in the area).

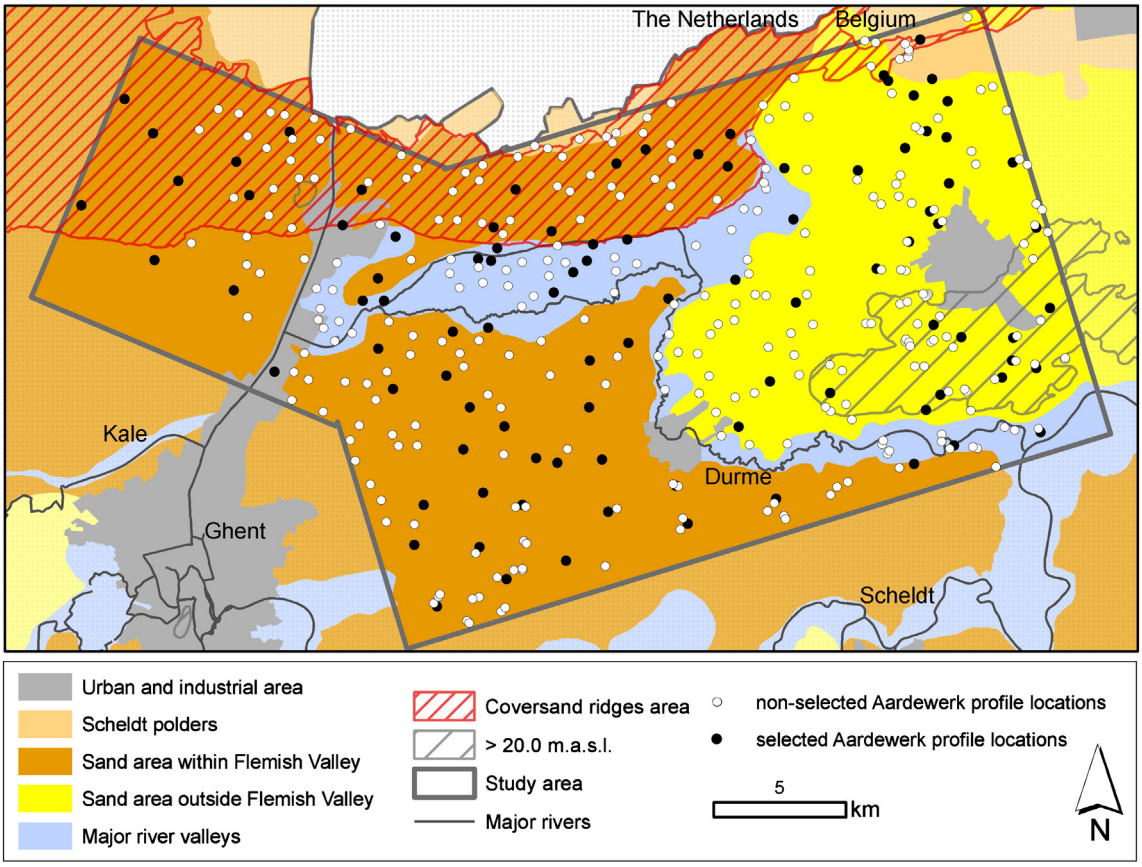

Fig. 2. Localization inside the study of the selected (solid black dots) and non-selected (solid white dots) profile locations area from the Aardewerk database. (For interpretation of the references to color in this figure legend, the reader is referred to the web version of this article.)

4.2. Parent material

Information on the initial soil conditions was estimated from the Aardewerk profile descriptions. The initial height of the soil profiles was corrected for material deposited on top of the soil in more recent times, such as plaggen and marine sediments. Their average thicknesses were deducted from the database and set at 0.40 m (no of locations = 15) and 0.50 m (no of locations = 1) for plaggen soils and locations subjected to marine influence and associated storm surges occurring in the 11th and 13th centuries (Soens, 2011), respectively. By removing these upper layers of the profile and reducing the height with this fixed value the initial profile height was reconstructed. However, the exact location and depth of the plaggen extraction zones are generally not provided in the literature. In general, it is assumed that around 10 ha of heath land was needed to provide the nutrients for 1 ha of arable land (FAO, 2001). Due to the unknown location of the extraction sites, and the relatively large extraction areas, a positive correction (adding heights, ca. 4 cm) was not applied.

The initial particle size distribution per profile location was taken from the C horizon recorded in the Aardewerk database. Furthermore, the OC content was adjusted for increasing values gained during soil formation and set at a predefined value of 0.1% in all layers. Only soil profiles with recorded peat presence, and soil layers with OC content not equal to 0.0% below 1.0 m, retained their original recorded OC content. To erase the influence of podzolization, the OC content of B and BC horizons, independent of their depth, was also set at 0.1%. As the Podzols have developed during the Holocene, this initial OC distribution is justified, but as podzolization is not simulated by SoilGen, this will cause a poor model evaluation at Podzol locations at the depths of the B-horizons. Initial $CaCO_3$ content was estimated from the cumulative distribution of the measured calcite content per (Belgian) texture class for all recorded horizons of the 390 Aardewerk profiles in the study area (Fig. 3). For all texture classes a large amount of samples with low calcite content was found, corresponding with decalcified samples (left tail of cumulative distributions, Fig. 3). Samples with high calcite content (>40.0%), especially in the sand loam, clay and heavy clay texture classes, reflect the presence of calcareous marls (located in the Moervaart depression, Fig. 1) or calcium-rich alluvial deposits (right tail of cumulative distributions, Fig. 3). The plateau of the cumulative distribution is not entirely flat, displaying the natural variation occurring at deposition and probably also the effect of calcite accumulation within the marls. The values at the left part of each plateau were assumed to represent the initial calcite content, resulting in 8.5% for the Belgian texture classes sand, loamy sand and light sand loam, and 13.0% for the texture classes loam, clay and heavy clay.

Initial CEC was conducted using a regression equation of Foth and Ellis (1996), that regressed CEC from OC and clay contents (in %; Eq. (1)) based on 5535 soil samples from a.o. continental U.S., Hawaii, Puerto Rico. A constant (f) was introduced to optimize and calibrate the equation for the local conditions of the study area. The value corresponding with the lowest RMSE between the estimated and measured (from Aardewerk database, no. of locations = 390) CECs was chosen as the final scaling-factor (f = 1.16) to calculate the initial CEC.

$$CEC = f \times (3.20 + 3.67 \times OC + 0.146 \times Clay). \quad (1)$$

The initial bulk density was calculated with the pedotransfer functions described by Wösten et al. (2001) based on a total of 863 measured soil characteristics in Dutch soils, using the reconstructed silt,

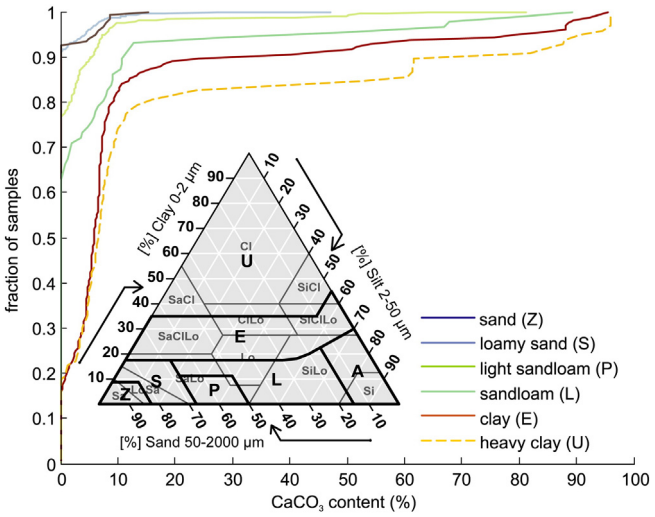

Fig. 3. Cumulative distribution function of the $CaCO_3$ content (%) as recorded for the 390 Aardewerk soil profiles located in the study area. A division is made per texture class (Belgian system) in order to assess the initial $CaCO_3$ content of the different parent materials. Texture triangle with Belgian classification system (black) and USDA classification system (gray) is inserted. For the explanation of the USDA abbreviations refer to Fig. 10. (For interpretation of the references to color in this figure legend, the reader is referred to the web version of this article.)

clay and OC contents, and the median of the sand fraction (M50). The latter was based on the median measurements of sandy layers recorded in the Aardewerk database (M50 = 145 µm). Finally, Gapon exchange constants (elements Al, Ca, K, Mg, Na and H) provided by De Vries and Posch (2003) for peat, clay, silt and sand and depths between 0.6 and 1.0 m, were assigned to each layer, based on the reconstructed fractions of OC and fine earth.

4.3. Climate

The SoilGen model requires yearly average January and July air temperatures and annual precipitation and potential evapotranspiration data as input (Fig. 4). These time series were calculated following the methods described in Finke and Hutson (2008). Present-day climate data used in these calculations were measured in the year 2005 at the weather station of Uccle in Belgium (50.8° N, 4.35° E). Temperature information on the entire simulation period was derived from area-averaged January and July air temperature anomalies, supplied by Davis et al. (2003). These anomaly series were produced for the most recent 12,000 years, in 100-year intervals, for 6 different regions encompassing Europe, based on quantitative pollen analyses (Davis et al., 2003). The January and July air temperature anomalies for central western Europe were converted towards local time series by adding actual measurements from the weather station. This discontinuous series was transformed by SoilGen into a continuous yearly values ($T_{Jan,y}$ and $T_{Jul,y}$) by linear interpolation between the 100-year intervals. Subsequently, a time series of weekly temperature data was calculated inside the model, using the continuous yearly time series and a standard time record of weekly temperature values from the weather station. The week values at this weather station for the months January and July were averaged ($T_{Jan,ws}$ and $T_{Jul,ws}$). For each year, the difference between $T_{Jan/Jul,y}$ and $T_{Jan/Jul,ws}$ was calculated, interpolated for the other months of the year and added to the weekly values of the standard record.

Annual precipitation anomalies for a time series covering the most recent 12,000 years in 100-year intervals were also provided by Davis (unpublished data), generated by the same method as described in Davis et al. (2003). By adding the current annual values from the weather station, the anomalies were converted to actual precipitation data. Equal to the temperature series, the SoilGen model linearly interpolated between the 100-year intervals, producing a yearly time series of annual precipitation. This yearly series was then used to

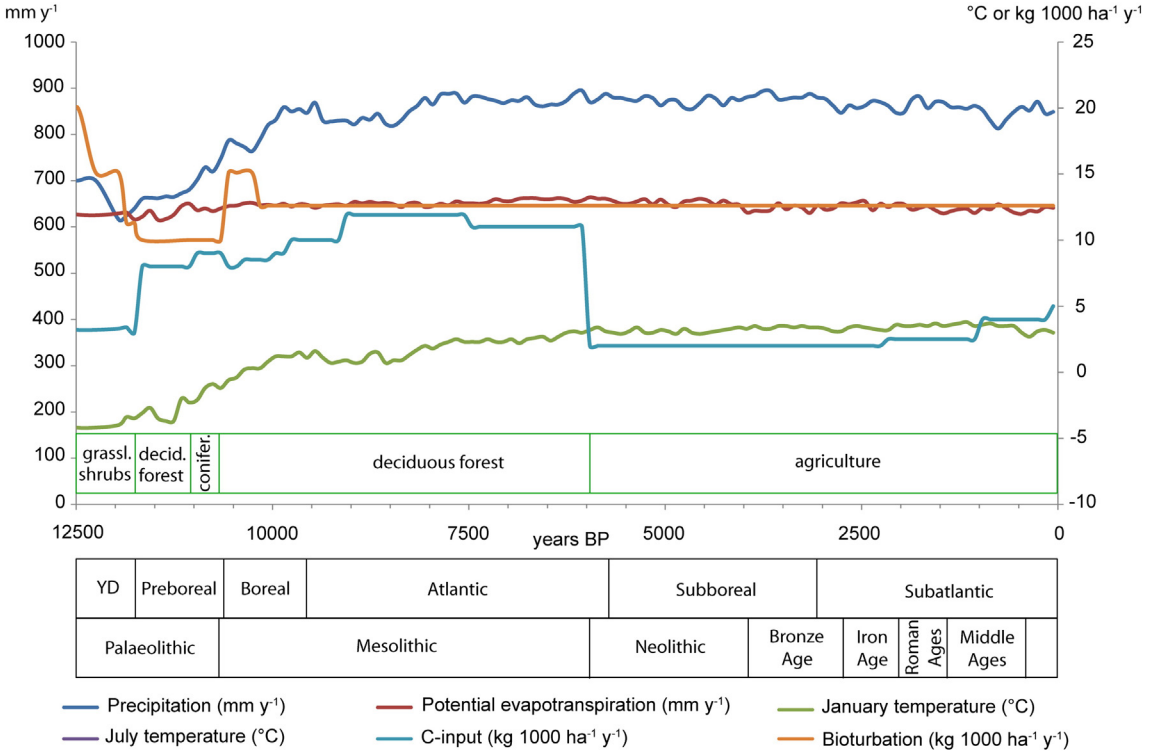

Fig. 4. The reconstructed boundary conditions related to climate, bioturbation and vegetation in function of the simulated time period. Vegetation types are: grassland (grassl.) and shrubs, deciduous forest (decid.), coniferous forest (conifer.) and agriculture. Chronostratigraphy and archeological periods are also indicated.

scale a standard record of daily precipitation data from the weather station, using a multiplier P_y/P_{ws}, in which P_y is the annual precipitation for the corresponding year in the precipitation time series and P_{ws} is the yearly precipitation measured at the weather station.

The equation of (Hargreaves and Samani, 1985) was used to calculate the daily potential evapotranspiration (ET_0) for 51° N, based on the average daily temperature and the temperature ranges from the weather station. A correction factor was obtained to calibrate the model, by comparing the yearly ET_0 measured at the weather station, with the yearly sum of calculated daily ET_0 values. Testing this calibrated model in a range of annual average temperatures, a linear regression function between ET_0 and the average yearly temperature was produced and used, together with the reconstructed temperature series, to construct a yearly ET_0 time series. The series was downscaled to a daily temporal resolution, by correcting the calculated daily ET_0 values for the weather station with a factor $ET_{0,y}/ET_{0,ws}$, where $ET_{0,y}$ is the yearly ET_0 at the corresponding year in the ET_0 time series and $ET_{0,ws}$ is the yearly ET_0 at the weather station.

4.4. Organisms

The vegetation history of the region was conceptualized by the 4 vegetation types present in the model (Fig. 4). Each type influences the interception evapotranspiration in varying orders (0% of the precipitation for grassland and shrubs and agriculture, 8% for deciduous forest and 12% for coniferous forest). Furthermore, the yearly leaf and root litter input were based on the dominant vegetation and reconstructed average July air temperatures and are provided to the model as a yearly time series (Fig. 4). The linear regression between July air temperatures and the litter production for the 4 vegetation types was based on the measurements for south-Norway from Sauer et al. (2012). The time series of the bioturbation (Fig. 4) is also directly related to the variations in vegetation type. Values concerning the minimum and maximum bioturbation depths and depth of the maximum bioturbation, together with the mass fractions of the solid phase mixed at the corresponding depths, were derived from vegetation related indicative values provided by Gobat et al. (1998) in the same manner as proposed by Finke and Hutson (2008).

Human influence by the means of agriculture was imposed in the model through the vegetation type agriculture and fertilization. From the Neolithic onward agriculture in the region became established, although most probably not in a continuous manner. Agriculture was applied in the model from 5960 BP onwards, although fertilization was only applied from 2560 BP (Iron Ages), similar to Finke and Hutson (2008; Belgian scenario). As from that year, the method of liming described by Plinius the Young was used (application of ~1 ton marl ac^{-1} per every 10 year, equal to 1.88 mol $CaCO_3$ m^{-2} every 10 years; Finke and Hutson, 2008). From 60 BP onwards, current liming management (0.276 mol $CaCO_3$ m^{-2} y^{-1}; Finke and Hutson, 2008) was assumed. The C-input to the soil by agricultural practice was implemented in the model by the introduction of the two-field crop rotation (from 2160 BP), three-field crop rotation (from 1060 BP), and modern agriculture (from 60 BP). C-inputs were obtained by estimating residues of barley in cropped years (using data from Finke and Goense, 1993) and biomass produced by weeds in set-aside years and taking a weighted average according to the rotation system.

4.5. Groundwater

The position of the groundwater table affects the drainage of the soil and its characteristics. For example, poorly drained soils often have less profile differentiation, higher OC and nitrogen contents, a lower pH and a higher Si to Al ratio than well-drained soil series under otherwise similar conditions (Jenny, 1941). The evolution of the mean water table for 30 year intervals was provided by Zwertvaegher et al. (2013), generated by a steady state groundwater modeling using 30 year averaged recharge data and adjusted topography and drainage network. The climate and vegetation data determining the recharge, were calculated in a similar manner as mentioned above. A continuous yearly series was obtained by a linear interpolation between the values. The mean water table was converted to the depth of a stagnating layer for SoilGen model calculations (see Section 3).

5. Model calibration

The decarbonization rate, influencing a.o. pH, porosity and cation content, was calibrated by adjusting the solubility constant of calcium carbonate (K_{SO}). Based on various soils in central Europe, normalized carbonate leaching rates (1.7–2.0 mol m^{-2} y^{-1} for coarse parent materials) for fixed soil water fluxes (1000 mm y^{-1}) where reported by Egli and Fitze (2001). By adjusting the K_{SO}, the number of simulated years necessary to decarbonize 1100 mm of a sandy parent material with a given $CaCO_3$ content under a leaching flux of 247 mm y^{-1} (high percolation value for the Holocene in the study area), was adapted to reproduce the necessary time for decarbonization defined by the metamodel of Egli and Fitze (2001). The K_{SO} with the highest comparison in decarbonization times between both models was chosen and afterwards used to evaluate model performance against the Egli and Fitze (2001) metamodel within a wider range of soil water fluxes.

6. Model performance evaluation

Model performance was evaluated by a comparison of the simulated values and the observed values as collected in the Aardewerk database, for the following variables: sand, silt and clay fractions (in mass% of fine earth), OC fraction (mass% of the solid fraction) and calcite mass fractions, pH and CEC ($mmol_c$ kg^{-1} soil). Measurements were only available for the final state. The final simulation year (1950) largely corresponds with the measurement years. These cover the years 1950–1953 ($n = 8, 29, 41, 11$, respectively), however a minor few are dating to 1962 ($n = 5$). Weighted averages for 4 zones of different depths were calculated: 0–0.4 m, 0.4–0.8 m, 0.8–1.2 m and 1.2 till the depth of the profile, which varied between the several locations. For the variable pH, the averages were calculated on the back-transformed concentrations, and afterwards recalculated towards the pH. In contrast to the other variables, the CEC in the Aardewerk database was not measured consistently for each layer and/or profile. This resulted in a comparison at only 88 locations compared to 96 locations for the other variables. The model performance was evaluated using three statistical deviance measures: the root mean square error (RMSE), giving the model's ability to accurately represent the observations, the mean error (ME) and the modeling efficiency (EF). The latter indicates the efficiency of the model in representing the measurements in accordance to their average value and gives an overall assessment of the goodness of fit (Mayer and Butler, 1993). In general, values of RMSE and ME should be close to 0 and close to 1 for the EF (Loague and Green, 1991).

7. From point scale to full-coverage

The simulated values at the different point locations were used to produce full-coverage maps of the target variables for the entire study period for a given year and depth range. As the maps are to be used for land evaluation purposes, they should reflect the condition of the topsoil. Therefore, the simulated values for the upper 0.4 m were combined and subsequently mapped. This mapping was achieved by performing a block (40 x 40 m^2) regression kriging in R (R Development Core Team, 2011) using several predictors (auxiliary maps) and based on the generic framework for spatial prediction as

proposed by Hengl et al. (2004). Target variables were chosen based on their relevance for past human occupation. These concerned sand, silt and clay fractions (%), OC content (%), calcite fraction (mass fraction), pH, base saturation (%) and bulk density (kg dm^{-3}). Following Hengl et al. (2004), the soil variables were standardized to a 0–1 scale and logit transformed, to improve the normality of the target variable. Further advantage of the standardization is that the predictions are bound to the physical range (Hengl, 2007; Hengl et al., 2004).

The used predictors are the elevation, the mean water table and the texture class, representing two continuous and one categorical variable, respectively. All maps were used on the spatial grain of 40 m by 40 m. This resolution was chosen in the light of future work, such as a land evaluation in which agricultural fields on the abovementioned grain are assumed to be reasonable (Zwertvaegher et al., 2010). Information on the elevation was present as a digital elevation model (DEM) of the study area. Depending on the chosen simulation year, a different DEM was used as a predictor. A present DEM, representative of the actual topography was originally produced by Werbrouck et al. (2011) on a 2 x 2 m^2 resolution and applied as a predictor map for years between 1804 CE (Common Era) and the present. A pre-medieval DEM, delivered by Werbrouck et al. (2011), in which anthropogenic artifacts

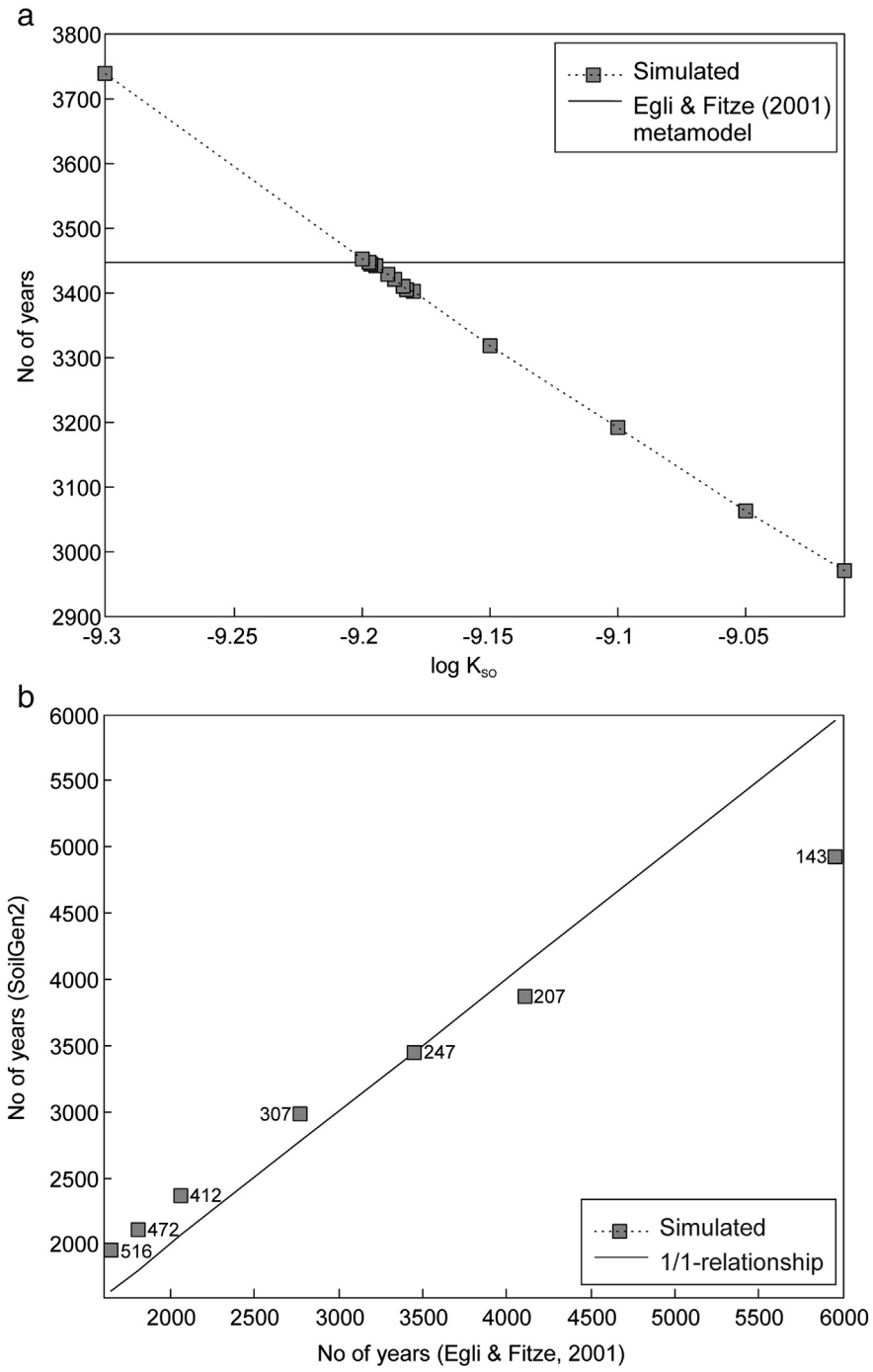

Fig. 5. a. Calibration of the solubility constant of calcite (log K_{SO}) under leaching conditions of 247 mm y^{-1}; b. comparison of the simulated number of years needed for decarbonization against the calculated values with the Egli and Fitze (2001) metamodel, under a range of varying leaching conditions: precipitation surplus of 143, 207, 247, 307, 412, 472 and 516 mm y^{-1}.

Table 1
Root mean square error (RMSE), mean absolute error (ME) and modeling efficiency (EF) for sand, silt, clay (mass% of fine earth) and OC (mass% of the solid fraction), calcite (mass fraction) and pH (all with n = 96), and CEC ($mmol_c\ kg^{-1}$ soil; n = 88) for zones of different depths beneath the surface (m). The total depth varies per profile location.

Variable	Depth beneath the surface (m)											
	0–0.4			0.4–0.8			0.8–1.2			1.2–end		
	RMSE	ME	EF	RMSE	ME	EF	RMSE	ME	EF	RMSE	ME	EF
Sand	5.85	3.40	0.89	1.84	1.06	0.99	0.98	0.66	1.00	3.09	−0.36	0.98
Silt	9.17	−8.39	0.35	2.25	−0.93	0.97	0.73	−0.24	1.00	1.78	−0.10	0.98
Clay	7.72	4.99	−0.17	1.41	−0.13	0.96	0.90	−0.42	0.98	2.55	0.47	0.90
OC	0.85	−0.21	0.28	0.35	0.14	−0.13	0.11	−0.04	0.48	0.08	−0.06	0.07
Calcite	0.07	0.01	0.25	0.09	0.02	−0.03	0.06	0.01	0.58	0.12	−0.08	−19.15
CEC	67.58	27.93	0.41	44.93	14.55	0.40	46.20	16.05	0.45	34.15	12.18	0.44
pH	1.09	0.49	−0.52	1.15	0.29	−0.43	1.19	0.44	−0.31	1.33	0.56	−0.32

were removed, was used for the years between 1114 CE and 1803 CE. For the years before 1114 CE, a (pre)historic DEM was used, in which plaggen layers and also marine sediments deposited during medieval storm surges and floodings were removed (Zwertvaegher et al., 2013).

In the same manner, the mean water table map of the specific year was also used as a predictor. These maps were produced by Zwertvaegher et al. (2013)on a 100 x 100 m^2 resolution and were afterwards downscaled to a 10 x 10 m^2 resolution following the method proposed by Sivapalan (1993) and Bierkens et al. (2000). Firstly, a regression relation was calculated based on the presently measured mean water table (Eq. (2); mwt_i in cm below surface) at 69 point locations in a pilot area of approximately 34 km^2 inside the current study area (Zidan, 2008) and on the present-day elevation (y_i in m, derived from the present DEM on 10 x 10 m^2 resolution).

$$mwt_i = b_0 + b_1 \times y_i. \quad (2)$$

This regression relation was assumed to be applicable to the entire study area and period. Based on this relation, combined with the weighted average mean water table (Eq. (3); *MWT* in cm below surface, per 100 x 100 m^2), the weighted average elevation (*Y* in m, per 100 x 100 m^2) and the elevation (y_i in m, per 10 x 10 m^2 cell), the mean water table for the 10 x 10 m^2 resolution (mwt_i in cm below surface) was calculated. Weighted averages were computed using a moving window surrounding the location *i*.

$$mwt_i = MWT-(b_1 \times Y) + b_1 \times y_i. \quad (3)$$

The predictor map on the texture classes was derived from the present-day soil map of Flanders (AGIV, the Flemish Geographical Information Agency). Following Hengl et al. (2004), this categorical layer was converted to binary (0–1) indicator maps. Due to the low amount of observations per separate texture class unit (minimum 5 observations per mapping unit; Hengl, 2009), combined with the

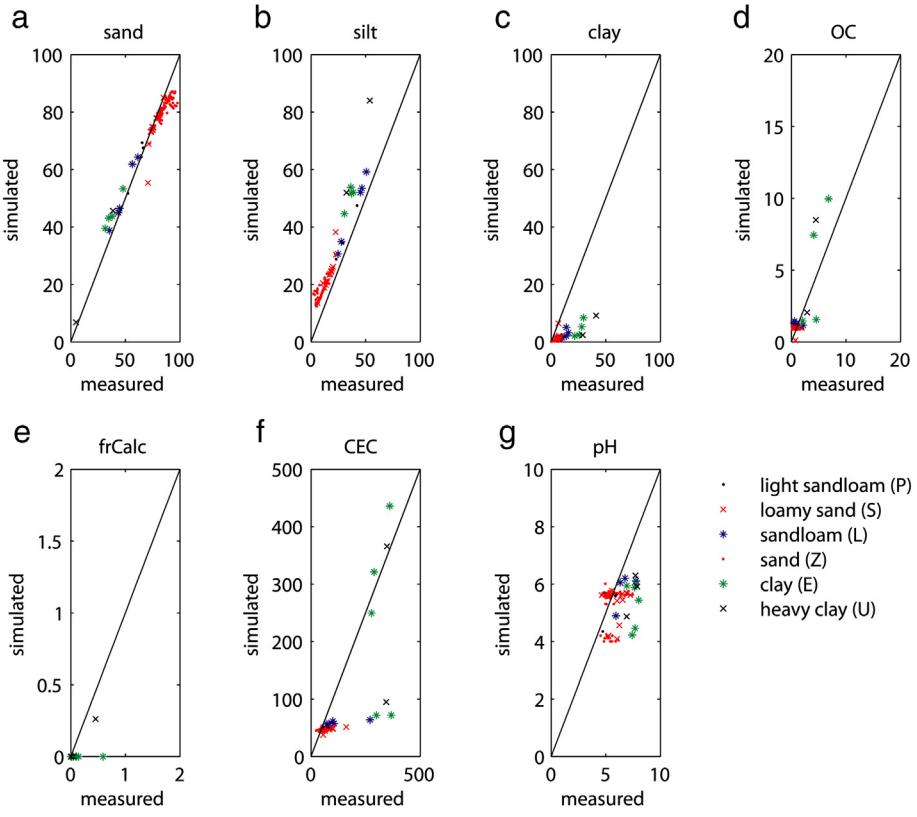

Fig. 6. Model performance evaluation for the upper 0.4 m of the profile. Weighted averages of the measured Aardewerk values are compared to the weighted averages of the simulated values for several soil variables: sand, silt and clay fractions in mass% of the fine earth fraction (a–b–c); OC in mass% of the solid fraction (d); calcite in mass fraction (e); CEC in $mmol_c\ kg^{-1}$ soil (f) and pH (g).

Table 2
Minimum, maximum and mean measured and predicted values of several soil variables up till 0.8 m depth. ZSP: Belgian texture classes sand (Z), sand loam (S) and light sand loam (P) grouped; LEU: Belgian texture classes loam (L), clay (E) and heavy clay (U) grouped. Units: sand, silt, clay in mass% of fine earth; OC in mass% of the solid fraction; calcite expressed as mass fraction; CEC in $mmol_c\ kg^{-1}$ soil.

ZSP	Depth beneath the surface (m)											
	0–0.4						0.4–0.8					
	Minimum		Maximum		Mean		Minimum		Maximum		Mean	
	Meas	Sim	Meas	Sim	Meas	Sim	Meas	Sim	Meas	Sim	Meas	Sim
Sand	52.38	51.66	97.75	89.06	84.22	79.79	54.38	54.71	99.00	97.74	86.64	86.06
Silt	2.25	10.75	42.25	47.42	11.76	19.37	0.55	1.61	39.75	40.49	9.72	10.40
Clay	0.00	0.12	11.58	6.47	4.02	0.84	0.00	0.54	12.25	11.93	3.64	3.54
OC	0.17	0.11	2.13	1.13	0.80	0.94	0.00	0.13	1.23	1.06	0.30	0.17
Calcite	0.00	0.00	0.01	0.00	0.00	0.00	0.00	0.00	0.34	0.00	0.01	0.00
CEC	23.38	37.82	161.75	51.69	61.84	46.53	25.13	36.23	105.50	59.59	54.41	46.87
pH	4.53	4.00	7.46	6.01	5.60	5.31	4.30	4.00	8.10	6.22	5.86	5.82
LEU	Depth beneath the surface (m)											
	0–0.4						0.4–0.8					
	Minimum		Maximum		Mean		Minimum		Maximum		Mean	
	Meas	Sim	Meas	Sim	Meas	Sim	Meas	Sim	Meas	Sim	Meas	Sim
Sand	4.88	6.81	61.50	70.71	39.74	45.25	1.75	1.32	93.88	92.20	53.11	57.76
Silt	24.75	27.72	54.00	83.99	38.65	50.02	3.25	3.69	56.63	57.41	32.52	28.05
Clay	9.63	1.47	41.13	17.05	21.61	4.74	1.00	2.27	52.13	55.58	14.37	14.18
OC	0.48	1.17	6.80	12.94	2.69	4.91	0.06	0.14	1.29	7.28	0.40	0.83
Calcite	0.00	0.00	0.59	0.26	0.11	0.02	0.00	0.00	0.59	0.41	0.11	0.03
CEC	72.88	56.49	367.88	558.45	243.20	215.13	35.13	42.52	341.25	377.77	138.29	91.30
pH	5.21	4.23	8.02	6.30	7.14	5.57	5.81	4.00	8.38	6.33	7.41	5.61

limited area occupied by these units in the study region, several classes were merged based on their affinity: the units heavy clay, clay, peat and marl, on the one hand and sandy loam and light sandy loam, on the other hand. Sand and loamy sand classes were taken as two separate categories. This resulted in 4 indicator maps. Together with the two earlier mentioned auxiliary maps, this led to a total of 6 predictor maps. To account for mutual independence between the auxiliary maps, a principal component analysis was performed on the predictors (Hengl et al., 2004). The resulting PCA maps were used in a step-wise multiple linear regression analysis (ordinary least squares method). Due to lack of an independent validation data set, the results were evaluated by a leave-one-out cross-validation (R gstat package; Pebesma, 2004), which was also performed for an ordinary kriging.

Based on the regression kriging maps of the sand, silt and clay fractions, a texture class map (USDA classification) of the topsoil was produced, using the classification method as provided by the R soil texture package from Moeys (2012).

8. Results and discussion

8.1. Calibration results

According to the Egli and Fitze (2001) metamodel, a total of 3446 years is necessary to decarbonize (leaching rate set at 1.95 mol $m^{-2}\ y^{-1}$) 1100 mm of a sandy profile with given carbonate content under leaching conditions of 247 mm y^{-1}. This time period was matched by the SoilGen model at a $\log(K_{SO})$ of 9.20 (Fig. 5a). Testing this value within a broader range of annual precipitation surpluses against the Egli and Fitze (2001) metamodel values (Fig. 5b) indicates that the SoilGen model simulates the decarbonization rather well at high precipitation surpluses, but overestimates the carbonate decarbonization rate at very low and very high surpluses, resulting in a RMSE (root mean square error) of 452 years. Very low values only occur at the beginning of the study period, from the Younger Dryas till the beginning of the Boreal. As can be derived from Fig. 4, very

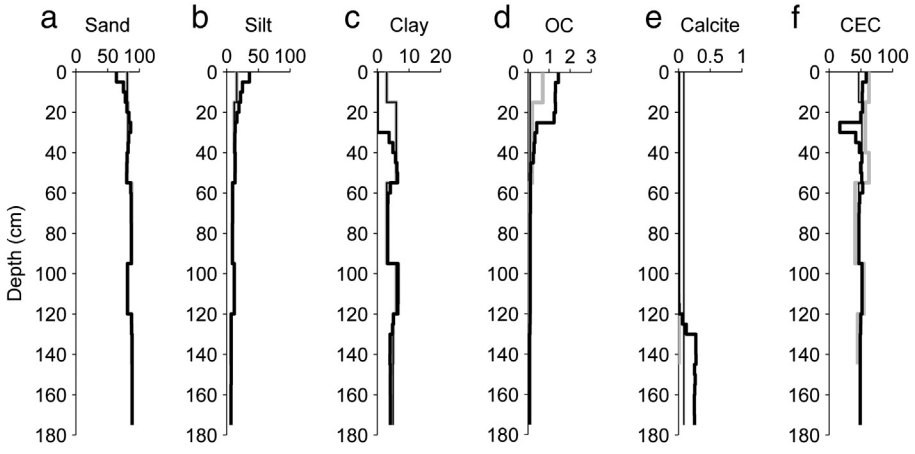

Fig. 7. Evolution of the initial (thin black line), measured (gray line) and simulated (bold black line) soil variables with depths: sand, silt and clay fractions in mass% of the fine earth fraction (a–b–c); OC in mass% of the solid fraction (d); calcite in mass fraction (e); CEC in $mmol_c\ kg^{-1}$ soil (f) and pH (g).

Table 3
Evaluation of the cross-validation on the ordinary (OK) and regression (RK) kriging performed on several logit transformed target soil variables for the year 12716 BP. Sand, silt and clay fractions expressed in mass% of the fine earth fraction; OC in mass% of the solid fraction; calcite as mass fraction; base saturation in %; bulk density expressed as kg dm^{-3}.

Variable	Explained variation (%)		RMSE	
	OK	RK	OK	RK
Sand	34.54	63.81	0.88	0.65
Silt	45.09	63.45	0.64	0.52
Clay	23.72	69.47	0.93	0.59
OC	9.01	44.80	0.65	0.50
Calcite	62.03	66.70	0.22	0.21
pH	−2.06	16.89	0.04	0.04
Base saturation	6.49	40.88	2.17	1.72
Bulk density	25.40	67.76	0.18	0.12

high precipitation surpluses (>350 mm y^{-1}) do not occur in the simulation period.

8.2. Predicted versus measured soil characteristics

Concerning the fine earth fractions, when considering all depths, the simulation results display an almost perfect fit with the measurements (EF close to 1; low RMSE and ME; Table 1; Fig. 6a–c). Only in the upper 0.4 m the model efficiency achieves worse than the global average concerning the clay fractions (Fig. 6c) and only slightly better, concerning the silt fractions (Fig. 6b; Table 1). Measured clay contents in the upper 0.4 m average around 4.0% (Table 2) in the texture group with coarser textured soils (Belgian texture classes Z, S and P grouped), and around 21.6% (Table 2) for the group with finer textures (Belgian texture classes L, E, U grouped). However, the simulated clay fractions for this upper zone, with averages at 0.8% (coarser texture classes) and 4.7% (finer texture classes) are lower than these measured values (Fig. 7c; Table 2). Furthermore, they are lower than the initial (estimated) values. Around a depth of 0.4 m, the simulated clay fraction reflects the measured one. This would suggest that the clay migration in the upper parts of the profile is overestimated by the model and exceeds the clay formation (probably by physical weathering), which might be also underestimated. The clay illuviation depth on the other hand is well predicted. Similar model trends on the prediction of the clay contents were also observed by Finke (2012) and Sauer et al. (2012).

The silt fraction in the 0.4 m of the profiles appears to be generally overestimated for all texture classes (Fig. 6b). The sand fraction, on the other hand, is slightly underestimated in the coarser and overestimated in the finer textured soil classes (Fig. 6a). Especially for the coarser textured soils this indicates that the weathering in the topsoil of the sand particles towards the silt fraction is overestimated by the model. Furthermore, the underestimation of the clay fraction affects the predicted sand and silt fractions in the opposite way.

Concerning the OC content, the EF indicates that the model performs rather well at all depth zones, except between 0.4 and 0.8 m. However, no clear trend is found: the deviation of the predicted

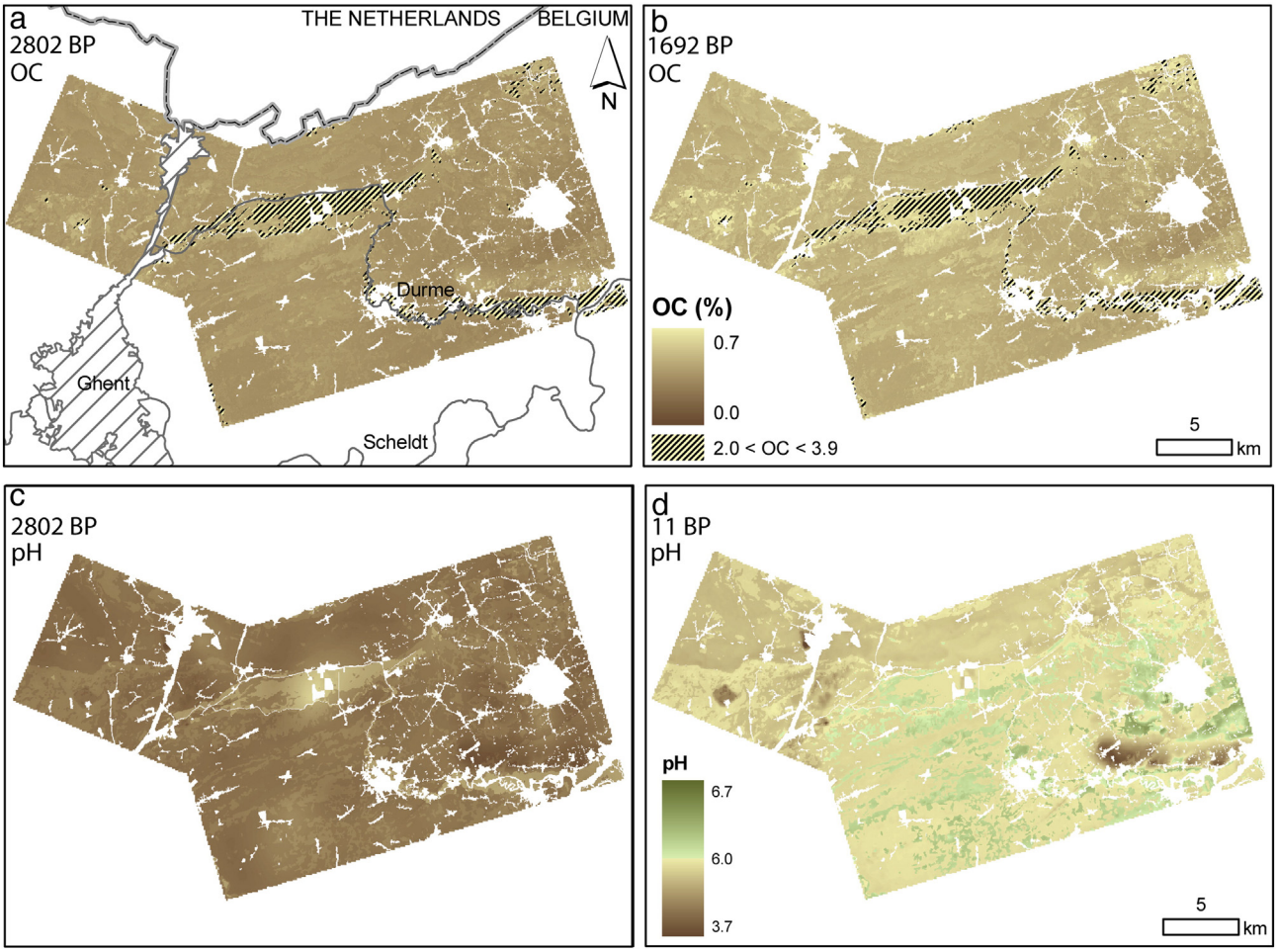

Fig. 8. Regression kriging maps of the OC content and the pH in the topsoil (0–0.4 m) for two different times. a. OC content at 2802 BP: prehistoric agriculture; b. OC content at 1692 BP: two-field crop rotation; c. pH at 2802 BP: prehistoric agriculture without liming; d. pH at 11 BP: modern agriculture and modern liming system.

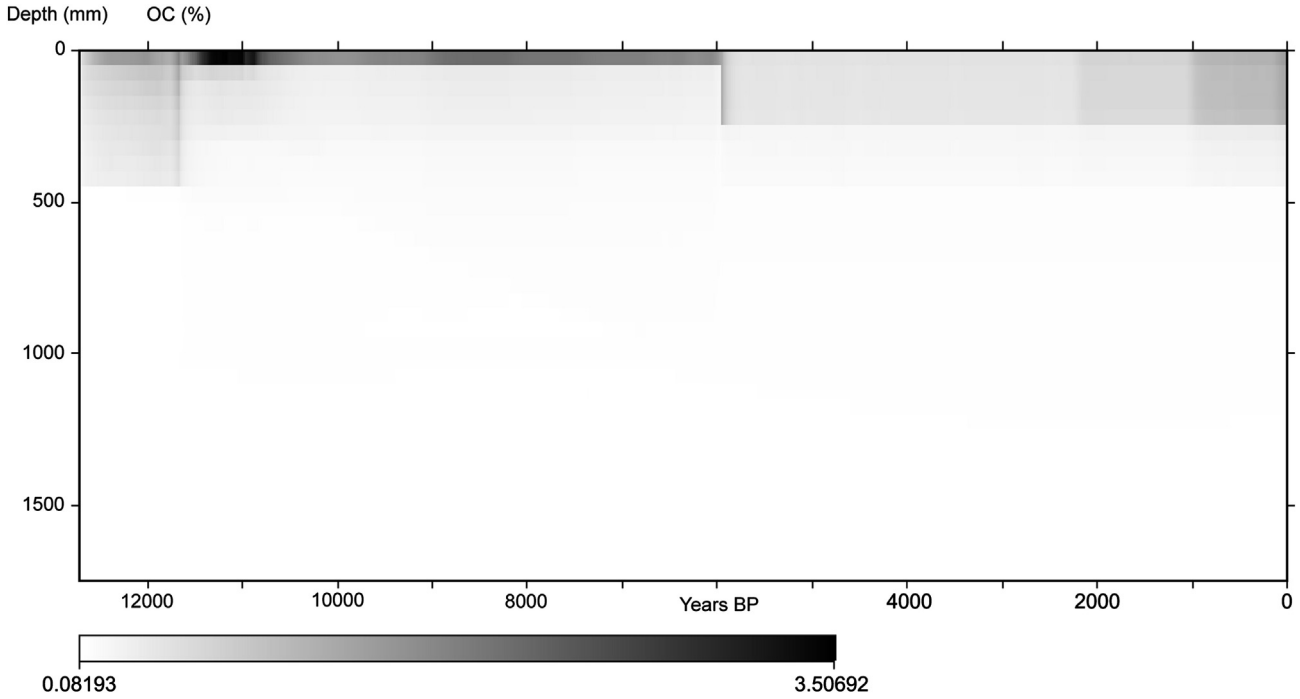

Fig. 9. Simulated evolution of the OC content (% of the solid fraction) at one location over the entire simulation period.

values from the measurements can be positive or negative. The general trend with depth, however, is as expected: predicted OC content in the topsoil at the final state is higher than the initial values, and decreases with increasing depth (Fig. 7d). The organic material applied to the topsoil is defined by the type of vegetation and in the final phase by the type of agriculture. Vegetation and agriculture type were administered uniform to all simulation locations, although this is not the case for the actual state. This might explain the non-consistent trend in OC deviation between predictions and measurements in the upper parts of the soil. Furthermore, several profiles are Podzols and characterized by elevated OC contents in the B horizon, generally appearing in the second depth zone (0.4–0.8 m). The podzolization process is however not yet included in the SoilGen model. This explains the underestimated OC contents and the worse model efficiency between 0.4 and 0.8 m depths.

Regarding the CEC, the model performs at all depth zones better than the overall average of the measurements (positive EF; Table 1). The average measured CEC in the top 0.4 m of the profiles is 61.8 $mmol_c\ kg^{-1}$ in the coarser textured soils and 243.2 $mmol_c\ kg^{-1}$ for the finer textured soils (Table 2). Generally, these measurements are underestimated by the model (Fig. 6f). Furthermore, at a 0.25–0.30 m depth, the model induces artifacts in the CEC depth profile at all locations (Fig. 7f). This is related to a drop in simulated OC at equal depths. Because the CEC is strongly related to the clay and OC contents, an underestimation of the CEC is to be expected whenever clay and/or OC content are also underestimated. This is what occurs at the 0.25–0.30 m profile depths.

The errors with respect to the calcite contents are low, but so is the actual calcite fraction (Table 2). The EF indicates a slightly better efficiency than the average of the measurements. The calcite accumulates at a certain depth, but the predicted accumulated fractions are often larger than the measured ones (Fig. 7e). In general, at present, most profiles are decalcified. This trend is also predicted by the model. However, a few locations still contain $CaCO_3$ (for example, a maximum of 60% in the upper 0.4 m of certain profiles) over their entire measured depth. These concern mostly marl deposits dating to the Late Glacial (Bats et al., 2011; Crombé, 2005) and even these modeled profiles are practically entirely decalcified. However, the solubility constant of calcite was calibrated (see Section 8.1.) and concluded to be adequate. This might suggest that during the simulation, although the calcite dissolution rate is estimated well, the dissolved calcite is too rapidly removed towards larger depths of the profile. This is most probably due to the enforced water table dynamics in the profiles, which appear to be overestimated. Underestimated calcite contents influence for example the pH and the base saturation. Considering the pH, the model performs generally worse than the global average of the measurements (negative EF). For the study area, the pH of the measurements ranges between 4.5 and 8.0 (Table 2) in the upper 0.4 m. This is however not matched by the simulations, where the profiles are on average too acid. This is especially true for the finer textured soil classes (Fig. 6g).

8.3. Full-coverage maps of soil variables at different points in time

The results of the regression kriging were compared with those of an ordinary kriging by performing a leave-one-out cross-validation, since no independent validation data set was at hand (Table 3). It must be mentioned however, that the cross-validation is in fact performed on point kriging and not on block kriging. Although the validation results are not in absolute terms applicable to the resulting maps, we believed that the observed relative trends are applicable to the performed block kriging. For all target variables, the amount of variation explained was the highest with the regression kriging, in these cases a better predictor than the ordinary kriging. Consistently, the RMSE on the regression kriging maps was also lower than for ordinary kriging. Furthermore, equal trends were found for other simulation years as well. However, the explained variation for pH, base saturation, OC and calcite contents can vary largely between simulation years and even can be rather low. We believe that this is most probably related to the data set: the simulation values as well as the profile location design. More accurate model predictions of the soil variables will most likely increase the accuracy of the kriging predictions. Furthermore, according to Hengl et al. (2004), a more

even distribution of the point data is more appropriate for regression kriging.

Besides the higher quality of the resulting maps in this case study, an additional advantage of regression kriging over ordinary kriging is that, due to the use of auxiliary maps, regional trends are displayed on the kriging maps. For example, as expected, the OC content predicted on the regression kriging maps of the upper 0.4 m of the soil (Fig. 8), is the highest in the areas bordering the rivers, while lower OC contents are predicted in the parts of the study area where sandy textured soils are dominant. More central in the study area, the Moervaart depression exhibits large OC contents as well. This area is characterized by clayey and loamy sediments, as well as peaty infillings and marls at certain places, representing alluvial and even former lacustrine environments. Therefore, the higher OC contents spatially predicted here, are also in line with the expectations.

Furthermore, similar trends are also displayed on the regression kriging maps considering more previous time periods (Fig. 8). They of course reflect the time evolution simulated at the separate point locations (Fig. 9). For example, high OC values of the upper 0.4 m such as the ones predicted for the Preboreal under natural vegetation conditions (Fig. 9), were strongly lowered due to the effect of prehistoric agriculture (Fig. 8a). The establishment of the two-field crop rotation system, applied in the model from 2160 BP (Late Iron Age) onwards, positively influenced the OC contents (Fig. 8b). It is a trend that was continued by the introduction of three-field crop rotation and modern type agriculture, because of its higher biomass production. Similarly, the effect of liming, introduced in the model from 2560 BP onwards, is expressed for example in the increase in pH (Fig. 8d). Again, regional trends are as expected: the highest values are found in the alluvial plains of the rivers and in the Moervaart depression, characterized by its marl infillings; the more acid values occur in the surrounding sandy sediments. The southern edge of the sand ridge of Maldegem–Stekene, were the leaching is the highest, reveals the lowest pH values. Very low pH values in the southeastern part of the study area are caused by overestimated groundwater depths (Zwertvaegher et al., 2013). However, as already said, the pH is underestimated by the model, resulting in too acid predictions at the profile locations, which is hence reflected in the full-coverage kriging maps. Furthermore, certain local hot spots (Fig. 8c) are found on the regression kriging map. Because regression kriging predicts the value of the target variable at the input location, this is related with inconsistencies in the target data, due to underestimated pH simulations. Better model predictions of the soil variables, will most likely result in better kriging predictions. Uncertainty maps will be useful in a later stage

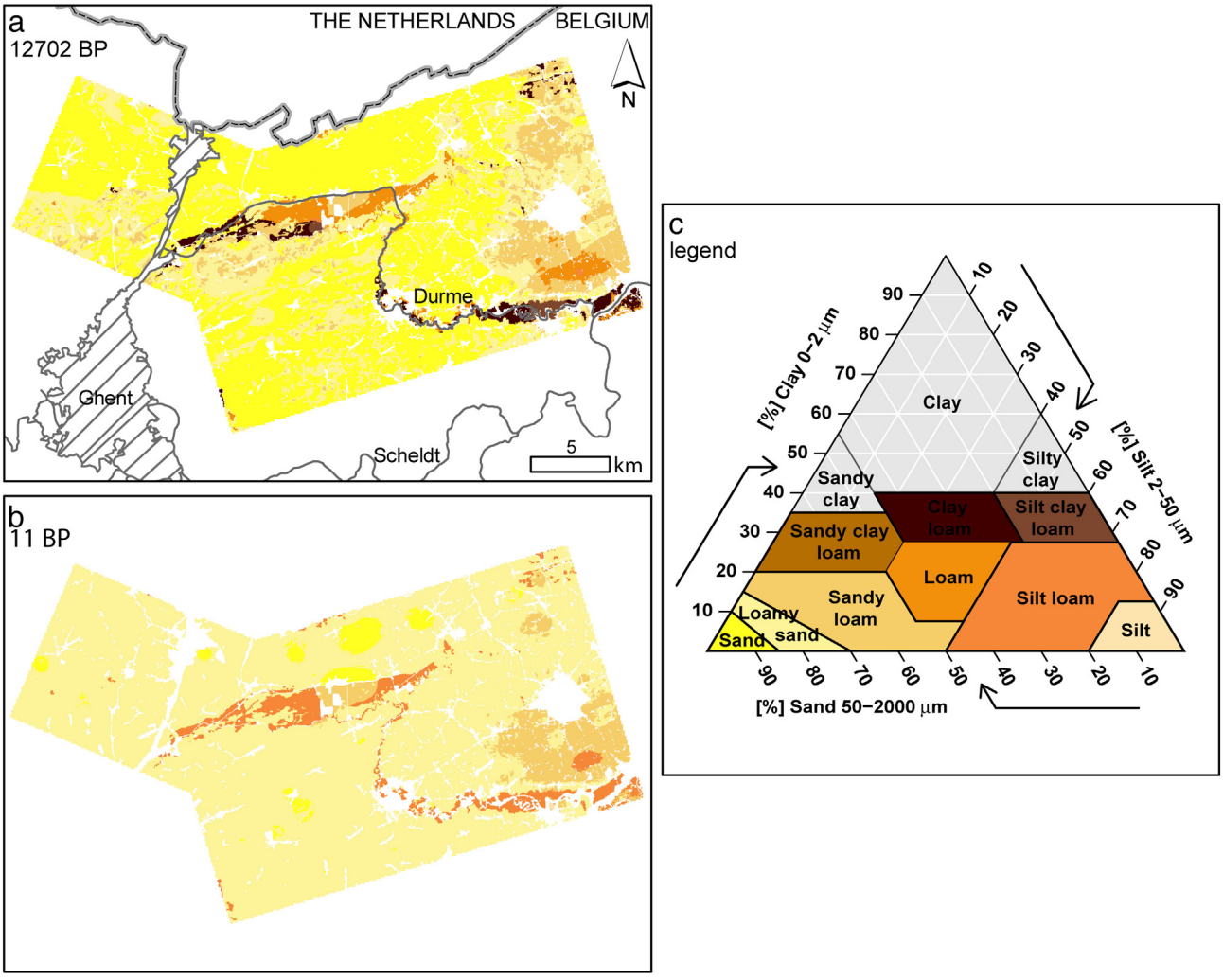

Fig. 10. Texture class maps of the topsoil (0–0.4 m) according to the USDA classification system based on the regression simulation results for the sand, silt and clay fractions at two different times. a. 12702 BP; b. 11 BP; c. USDA texture triangle explaining the used color codes. (For interpretation of the references to color in this figure legend, the reader is referred to the web version of this article.)

when the effect of combined uncertainties needs to be estimated on interpretive maps like soil suitability maps for prehistoric agriculture, or on population support capacity estimates.

The predictions on the fine earth fractions were used to create topsoil texture class maps according to the USDA soil texture classification system (Fig. 10). Again, regional patterns are observed: finer textured soils in the alluvial valleys, while the rest of the study area is largely characterized by a coarser material. However, for the most recent period (Fig. 10b), textures are not entirely consistent with what can be found on the present day soil map. This is related to the simulations, were weathering was overestimated as well as clay migration, resulting in an underestimation of the sand and clay fractions and an overestimation of the silt fraction.

9. Conclusions

The SoilGen2 model was used to predict the evolution of several soil variables at various depths at 96 profile locations in a 584 km^2 study area in Sandy Flanders (Belgium). A time period of 12,716 years was covered, starting in the Younger Dryas and spanning the entire Holocene. The model quality was optimized by calibration of the calcite solubility constant and testing the calibrated value under a wide range of representative precipitation surpluses. The model performance evaluation indicated that the fine earth fractions were reasonably well predicted. However, clay fractions in the upper part of the soil were strongly underestimated, due to overestimation of the clay migration, while clay formation might be underestimated. On the other hand, the illuviation depth was estimated well. Sand and silt fractions were respectively under- and overestimated, as the result of an overestimation of the weathering. CEC, calcite content and pH were underestimated. The model quality can therefore be optimized by focusing on these processes. Additionally, errors may have been introduced by poor estimates of initial soil properties in the Younger Dryas. Adding the podzolization process as well, will enhance the OC estimations at higher depths in these coarser textured soils. Furthermore, the mimicked dynamics of shallow water tables falling within the profile, need to be re-examined. Of course, one must keep in mind that a better reconstruction of the boundary conditions can also improve model quality. However, the necessary data are not always available. For example, in sandy grounds, pollen and archeological evidence, are often badly preserved.

The use of a regression kriging framework, as proposed by Hengl et al. (2004) on the simulated point locations, enabled the creation of full-coverage maps of several soil characteristics at certain points in time. The regional variation on the regression kriging maps, reflected well the expected trend. The results can be optimized by using a more equally distributed point data set (Hengl et al., 2004). Furthermore, increased model quality will most probably also affect the regression kriging. Hengl et al. (2004) point out that the methodology on the spatial prediction of soil variables can be extended by including temporal variability of soil variables, as well as their variability with depth. We believe the SoilGen model, combined with the regression kriging framework, is a step in answering this question. Future research for other appropriate and/or improved auxiliary maps seems at hand, especially for internal (in depth) kriging predictions.

Maps of soil properties and associated uncertainty for past situations are useful to display past soilscapes and analyze these in terms of suitability for (pre-)historic agriculture and thus explain variations in population density.

Acknowledgements

The authors gratefully acknowledge the Ghent University Integrated Project BOF08/GOA/009 “Prehistoric settlement and land-use systems in Sandy Flanders (NW Belgium): a diachronic and geo-archeological approach” for financially supporting this work. Our thanks go to B. Davis for supplying the January and July temperature anomaly data for central-western Europe and the precipitation data for the same regions. We also thank A. Frankl for his help with some figures.

References

Addiscott, T.M., Wagenet, R.J., 1985. Concepts of solute leaching in soils — a review of modeling approaches. Journal of Soil Science 36 (3), 411–424.
Ameryckx, J., 1960. La pédogenèse en Flandre sablonneuse. Pédologie 10, 124–190.
Bats, M., De Smedt, P., De Reu, J., Gelorini, V., Zwertvaegher, A., Antrop, M., De Maeyer, P., Finke, P.A., Van Meirvenne, M., Verniers, J., Crombé, P., 2011. Continued geoarchaeological research at the Moervaart palaeolake area (East Flaners, B): field campaign 2011. Notae Praehistoricae 31, 201–211.
Bierkens, M.F.P., Finke, P.A., de Willigen, P., 2000. Upscaling and Downscaling Methods for Environmental Research. Kluwer Academic Publishers, Dordrecht.
Blume, H.-P., Leinweber, P., 2004. Plaggen soils: landscape history, properties, and classification. Journal of Plant Nutrition and Soil Science 167, 319–327.
Coleman, K., Jenkinson, D.S., 2005. ROTHC-26.3. A model for the Turnover of Carbon in Soil. Model Description and Windows Users Guide (November 1999 issue (modified April 2005), Harpenden, UK).
Crombé, P., 2005. The last hunter–gatherer–fishermen in Sandy Flanders (NW Belgium). The Verrebroek and Doel excavation projects. Vol. 1. Archaeological Reports Ghent University, 3. Ghent University, Gent.
Crombé, P., Vanmontfort, B., 2007. The neolithisation of the Scheldt and Basin in western Belgium. Proceedings of the British Academy 144, 261–283.
Crombé, P., Van Strydonck, M., Boudin, M., Van den Brande, T., Derese, C., Vandenberghe, D., Van den haute, P., Court-Picon, M., Verniers, J., Gelorini, V., Bos, J.A.A., Verbruggen, F., Antrop, M., Bats, M., Bourgeois, J., De Reu, J., De Maeyer, P., De Smedt, P., Finke, P.A., Van Meirvenne, M., Zwertvaegher, A., 2012. Absolute dating (14C and OSL) of the formation of coversand ridges occupied by prehistoric hunter–gatherers in NW Belgium. Radiocarbon 54, 715–726.
Dann, R.L., Close, M.E., Lee, R., Pang, L., 2006. Impact of data quality and model complexity on prediction of pesticide leaching. Journal of Environmental Quality 35 (2), 628–640.
Davis, B.A.S., Brewer, S., Stevenson, A.C., Guiot, J., Contributors, D., 2003. The temperature of Europe during the Holocene reconstructed from pollen data. Quaternary Science Reviews 22, 1701–1716.
De Moor, G., Heyse, I., 1974. Lithostratigrafie van de Kwartaire afzettingen in de overgangszone tussen de kustvlakte en de Vlaamse Vallei in Noordwest België. Natuurwetenschappelijk Tijdschrift 56, 85–109.
De Moor, G., van de Velde, D., 1995. Toelichting bij de Quartairgeologische Kaart. Kaartblad 14: Lokeren. Universiteit Gent, Ministerie van de Vlaamse Gemeenschap — Afdeling Natuurlijke Rijkdommen en Energie, Brussel.
De Reu, J., Bourgeois, J., De Smedt, P., Zwertvaegher, A., Antrop, M., Bats, M., De Maeyer, P., Finke, P.A., Van Meirvenne, M., Verniers, J., Crombé, P., 2011. Measuring the relative topographic position of archaeological sites in the landscape, a case study on the Bronze Age barrows in northwest Belgium. Journal of Archaeological Science 38, 3435–3446.
De Vries, W., Posch, M., 2003. Derivation of cation exchange constants for sand, loess, clay and peat soils on the basis of field measurements in the Netherlands. Alterra-report, 701. Alterra Green World research, Wageningen.
Dudal, R., Deckers, J., Van Orshoven, J., Van Ranst, E., 2005. Soil Survey in Belgium and Its Applications.
Egli, M., Fitze, P., 2001. Quantitative aspects of carbonate leaching of soils with differing ages and climates. Catena 46, 35–62.
FAO, 2001. Mixed crop-livestock farming. A review of traditional technologies based on literature and field experience. FAO Animal production and health papers, 152. FAO, Rome.
Finke, P.A., 2012. Modeling the genesis of luvisols as a function of topographic position in loess parent material. Quaternary International 266, 3–17.
Finke, P.A., Goense, D., 1993. Differences in barley grain yields as a result of soil variability. Journal of Agricultural Science 120, 171–180.
Finke, P.A., Hutson, J.L., 2008. Modelling soil genesis in calcareous loess. Geoderma 145, 462–479.
Finke, P.A., Meylemans, E., Van de Wauw, J., 2008. Mapping the possible occurrence of archaeological sites by Bayesian inference. Journal of Archaeological Science 35 (2008), 2786–2796.
Finke, P.A., Vanwalleghem, T., Opolot, E., Poesen, J., Deckers, J., 2013w. Estimating the Effect of Tree Uprooting on Variation of Soil Horizon Depth by Confronting Pedogenetic Simulations to Measurements in a Belgian Loess Area (in review).
Foth, H.D., Ellis, B.G., 1996. Soil Fertility, 2nd ed. CRC Press, Lewis 304.
Gobat, J.-M., Aragno, M., Matthey, W., 1998. Le sol vivant. Press polytechniques et universitaires romandes, Lausanne.
Hargreaves, G.H., Samani, Z.A., 1985. Reference crop evapotranspiration from temperature. Applied Engineering in Agriculture 1, 96–99.
Hengl, T., 2007. A practical guide to geostatistical mapping of environmental variables. EUR 22904. Scientific and Technical Research Series. Office for Official Publications of the European Communities, Luxemburg.
Hengl, T., 2009. A Practical Guide to Geostatistical Mapping. www.lulu.com (Amsterdam).
Hengl, T., Heuvelink, G.B.M., Stein, A., 2004. A generic framework for spatial prediction of soil variables based on regression-kriging. Geoderma 120, 75–93.

Heyse, I., 1979. Bijdrage tot de geomorfologische kennis van het Noordwesten van Oost-Vlaanderen. verhandelingen van de koninklijke Academie voor Wetenschappen, letteren en schone kunsten van België, Klasse der wetenschappen. Paleis der Academiën, Brussel.
Hutson, J.L., Wagenet, R.J., 1992. LEACHM: Leaching Estimation and Chemistry Model: A Process Based Model of Water and Solute Movement Transformations, Plant Uptake and Chemical Reactions in the Unsaturated Zone, vol. 2. Water Resources Inst., Cornell University, Ithaca, NY (Version 3).
IUSS Working Group WRB, 2006. World reference base for soil resources 2006. A framework for international classification, correlation and communication. World Soil Resources Report, No. 103. FAO, Rome.
Jabro, J.D., Jabro, A.D., Fox, R.H., 2006. Accuracy and performance of three water quality models for simulating nitrate nitrogen losses under corn. Journal of Environmental Quality 36 (4), 1227–1236.
Jalali, M., Rowell, D.M., 2003. The role of calcite and gypsum in the leaching of potassium in a sandy soil. Experimental Agriculture 39, 379–394.
Jenny, H., 1941. Factors of Soil Formation. A System of Quantitative Pedology. McGraw-Hill Book Company, Inc., New York 281.
Knight, D., Howard, A.J., 2004. Trent Valley Landscapes. The Archaeology of 500,000 Years of Change. Heritage Marketing and Publications Ltd, King's Lynn.
Loague, K., Green, R.E., 1991. Statistical and graphical methods for evaluating solute transport models: overview and application. Journal of Contaminant Hydrology 7, 51–73.
Mayer, D.G., Butler, D.G., 1993. Statistical validation. Ecological Modelling 68, 21–32.
Moeys, J., 2012. The Soil Texture Wizard: R Functions for Plotting, Classifying, Transforming and Exploring Soil Texture Data.
Niknami, K.A., Amirkhiz, A.C., Jalali, F.F., 2009. Spatial pattern of archaeological site distribution on the eastern shores of Lake Urmia, northwestern Iran. Archeologia e Calcolatori 20, 261–276.
Oetelaar, G.A., Oetelaar, J., 2007. The new ecology and landscape archaeology: incorporating the anthropogenic factor in models of settlement systems in the Canadian prairie ecozone. Canadian Journal of Archaeology 31, 65–92.
Opolot, E., Yu, Y.Y., Finke, P.A., 2013w. Modeling Soil Genesis at Pedon and Landscape Scales: Achievements and Problems (in review).
Pebesma, E., 2004. Computers and Geosciences 30, 683–691.
R Development Core Team, 2011. R: A Language and Environment for Statistical Computing. R Foundation for Statistical Computing, Vienna, Austria.
Samouëlian, A., Finke, P., Goddéris, Y., Cornu, S., 2012. Hydrologic Information in pedologic models. In: Lin, H. (Ed.), Hydropedology: Synergistic Integration of Pedology and Hydrology. ISBN: 9780123869418, pp. 595–636.
Sanders, J., Sys, C., Vandenhout, H., 1989. Bodemkaart van België — Verklarende tekst bij het kaartblad Stekene 26E. Centrum voor de afwerking van de Bodemkaart in het Noorden van het land.
Sauer, D., Finke, P.A., Sørensen, R., Sperstad, R., Schülli-Maurer, I., Høeg, H., Stahr, K., 2012. Testing a soil development model against southern Norway soil chronosequences. Quaternary International 265, 18–31.
Sivapalan, M., 1993. Linking hydrologic parameterizations across a range of scales: hill slope to catchment to region. Exchange Processes at the Land Surface for a Range of Space and Time Scales. Proceedings of the Yokohama Symposium. IAHS Publ., pp. 115–123.
Smith, P., Smith, J.U., Powlson, D.S., McGill, W.B., Arah, J.R.M., Chertob, O.G., Coleman, K., Franko, U., Frolking, S., Jenkinson, D.S., Jensen, L.S., Kelly, R.H., Klein-Gunnewiek, H., Komarov, A.S., Li, C., Molina, J.A.E., Mueller, T., Parton, W.J., Thornley, J.H.M., Whitmore, A.P., 1997. A comparison of the performance of nine soil organic matter models using datasets from seven long-term experiments. Geoderma 81 (1–2), 153–225.
Soens, T., 2011. The genesis of the Western Scheldt: towards an anthropogenic explanation for environmental change in the medieval Flemish coastal plain (1250–1600). In: Thoen, E., Borger, G., Soens, T., De Kraker, A.M.J., Tys, D., Vervaet, L. (Eds.), Landscapes or Seascapes? The History of the Coastal Area in the North Sea Region Revised: CORN Publication Series Brepols Publishers, Turnhout.
Tavernier, R., Maréchal, R., Ameryckx, J., 1960. Bodemkartering en bodemklassifikatie in België. Ministerie van Landbouw, Nationaal Comité van FAO.
Van Orshoven, J., Maes, J., Vereecken, H., Feyen, J., Dudal, R., 1988. A structured database of Belgian soil profile data. Pédologie 38 (2), 191–206.
Van Orshoven, J., Deckers, J.A., Vandenbroucke, D., Feyen, J., 1993. The completed database of Belgian soil profile data and its applicability in planning and management of rural land. Bulletin des Recherches Agronomiques de Gembloux 28, 197–222.
Van Ranst, E., Sys, C., 2000. Eenduidige legende voor de digitale bodemkaart van Vlaanderen. Universiteit Gent, Gent.
Vanwalleghem, T., Stockmann, U., Minasny, B., McBratney, A.B., 2013. A quantative model for integrating landscape evolution and soil formation. Journal of Geophysical Research — Earth Surface. http://dx.doi.org/10.1002/jgrf.20026 (in press).
Verbruggen, C., 1971. Postglaciale landschapsgeschiedenis van zandig Vlaanderen. Botanische, ecologische en morfologische aspekten op bais van palynologisch onderzoek. Rijksuniversiteit Gent.
Verbruggen, C., Denys, L., Kiden, P., 1996. Belgium. In: Berglund, B.E., Birks, H.J.B., Ralska-Jasiewiczowa, M., Wright, H.E. (Eds.), Palaeoecological Events during the Last 15000 Years: Regional Syntheses of Palaeoecological Studies of Lakes and Mires in Europe. John Wiley & Sons, Chichester, pp. 553–574.
Werbrouck, I., Antrop, M., Van Eetvelde, V., Stal, C., De Maeyer, P., Bats, M., Bourgeois, J., Court-Picon, M., Crombé, P., De Reu, J., De Smedt, P., Finke, P.A., Van Meirvenne, M., Verniers, J., Zwertvaegher, A., 2011. Digital elevation model generation for historical landscape analysis based on LiDAR data, a case study in Flanders (Belgium). Expert Systems with Applications 38, 8178–8185.
Wösten, J.H.M., Veerman, G.J., De Groot, W.J.M., Stolte, J., 2001. Waterretentie- en doorlatendheidskarakteristieken van boven- en ondergronden in Nederland: de Staringreeks. Alterra, Wageningens.
Zidan, Y.O.Y., 2008. Mapping phreatic water tables to update the drainage class map 1:20,000 in the Scheldt Valley near Ghent. Unpublished thesis. Thesis submitted in partial fulfillment of the requirements for the degree of Master of Science in Physical Land Resources Thesis, Ghent University, Ghent, 89 pp.
Zwertvaegher, A., Werbrouck, I., Finke, P.A., De Reu, J., Crombé, P., Bats, M., Antrop, M., Bourgeois, P., Court-Picon, M., De Maeyer, P., De Smedt, P., Sergant, J., Van Meirvenne, M., Verniers, J., 2010. On the use of integrated process models to reconstruct prehistoric occupation, with examples from Sandy Flanders, Belgium. Geoarchaeology: An International Journal 25 (6), 784–814.
Zwertvaegher, A., Finke, P.A., De Reu, J., Vandenbohede, A., Lebbe, L., Bats, M., De Clercq, W., De Smedt, P., Gelorini, V., Sergant, J., Antrop, M., Bourgeois, J., De Maeyer, P., Van Meirvenne, M., Verniers, J., Crombé, P., 2013. Reconstructing phreatic palaeogroundwater levels in a geoarchaeological context, a case study in Flanders (Belgium). Geoarchaeology: An International Journal 28, 170–189.